Hydrogen release from hydrolysis of $NaBH_4$-NH_3BH_3 composite promoted by $CoCl_2 \cdot 6H_2O$

M. Yang[a], Y. C. Wu[a], Y. H. Liu[a], J. Q. Chen[a], C. L. Wu[b], W. Feng[a,c,d], W. T. Cai[e,f], X. L. Wang[a,c,d,*]

[a]*School of Mechanical Engineering, Chengdu University, Chengdu 610106, PR China*

[b]*Engineering Research Center of Alternative Energy Materials & Devices, Ministry of Education, Sichuan University, Chengdu 610065, PR China*

[c]*Sichuan Province Engineering Technology Research Center of Powder Metallurgy, Chengdu University, Chengdu 610106, PR China*

[d]*Institute for Advanced Study, Chengdu University, Chengdu 610106, PR China*

[e]*School of Materials and Energy, Guangdong University of Technology, Guangzhou 510006, PR China*

[f]*Guangdong Provincial Key Laboratory of Advanced Energy Storage Materials, South China University of Technology, Guangzhou 510006, PR China*

In recent years, the effective hydrogen release from hydrogen storage materials has attracted extensive attention. In this work, $CoCl_2 \cdot 6H_2O$ (Cobalt chloride hexahydrate, CCH), a low cost and easily available catalyst, was successfully used to catalyze the hydrolysis of $NaBH_4$-NH_3BH_3 composite (xSB-AB, x is the molar ratio of SB to AB). The results show that the synergistic effect produced by ball milling is beneficial to improve the hydrogen release performance of xSB-AB hydrolysis. This work not only advances the understanding of the synergistic effect of SB and AB, but also provides a basis for using low-cost catalysts to improve the hydrolysis performance of xSB-AB.

(Received April 23, 2023; Accepted July 27, 2023)

Keywords: Hydrolysis, Hydrogen release, $NaBH_4$, NH_3BH_3, $CoCl_2 \cdot 6H_2O$

1. Introduction

With the exhaustion of fossil fuels and the increasingly severe environmental pollution, it is very urgent and significant to develop a sustainable new energy source [1-3]. As a clean and abundant energy carrier, hydrogen is considered to be the most potential fossil fuel substitute in the future. However, how to store and transport hydrogen is still a challenge [4-6], which also limits its application in energy devices such as fuel cells [7]. Therefore, it is extremely important to develop a cost-effective hydrogen storage technology [8]. Compared with high-pressure gaseous and liquid hydrogen storage, solid hydrogen storage has the advantages of high volumetric storage density, low working pressure and good safety performance [9]. Among many solid hydrogen

* Corresponding author: wangxiaolian@cdu.edu.cn
https://doi.org/10.15251/DJNB.2023.183.899

storage materials, sodium borohydride ($NaBH_4$, SB) [1, 10, 11] and ammonia borane (NH_3BH_3, AB) [12, 13] have become research hotspots in recent years due to the advantages of high theoretical hydrogen storage density, good stability at room temperature, easy storage and transportation. They can release hydrogen through pyrolysis and hydrolysis. However, the pyrolysis method has problems such as high dehydrogenation temperature, difficult reaction control [14], and release of toxic substances [15]. In contrast, hydrolysis has the advantages of mild reaction conditions and easy control [16]. The hydrolysis reaction of SB and AB are respectively described as formula (1) and (2).

$$NaBH_4(aq) + 2H_2O(l) \rightarrow Na^+(aq) + BO_2^-(aq) + 4H_2(g) \quad (1)$$

$$NH_3BH_3(aq) + 2H_2O(l) \rightarrow NH_4^+(aq) + BO_2^-(aq) + 3H_2(g) \quad (2)$$

The hydrogen release rate of SB and AB monomer hydrolysis is very slow, and the hydrogen yield (HY) is also not ideal. For example, the hydrogen release of SB and AB after reacting with water for 1 h at room temperature is only about 2.17 wt% and 2.10 wt%, respectively [5]. Therefore, it is necessary to find an efficient and economical catalyst. Noble metal catalysts, such as Pt [14, 17], Au [18], Ru [19-21], and Rh [22, 23] have a good catalytic effect on the hydrolysis of SB and AB. However, the high cost of noble metal catalysts and insufficient reserves limit its application [24]. Non-noble metal catalysts occupy an increasingly higher position, because it has advantages of low cost, abundant reserves, and high catalytic activity [25-27]. Because of the simple preparation and high catalytic activity for the hydrolysis of SB and AB [8, 28], Co-based catalysts, such as Co nanoparticles [29, 30], Co-B [31], Co-Ni [16], Co-Cu-B [32, 33], Co-Fe/Mn-B [34] and Co-Fe-Ru-B[35] have been widely studied. Çetin Çakanyildirim et al. [36] found that that a $CoCl_2$ catalyst loaded on a carrier containing γ-Al_2O_3 can be used continuously for 250 h. The activation energies of the catalytic hydrolysis of $NaBH_4$ at low temperature (20-40 ℃) and high temperature (50-65 ℃) are 132 $kJ \cdot mol^{-1}$ and 78$\cdot kJ \cdot mol^{-1}$, respectively. In addition, the hydrolysis of $NaBH_4$ with different amounts of $CoCl_2$ catalysts supported by activate carbon also have good catalytic performance, and the activation energy is 48 $kJ \cdot mol^{-1}$ [37]. Sait Izgi et al. [38] supported Co-Cr-B catalyst on γ-Al_2O_3, which catalyzed the hydrolysis of NH_3BH_3 with a hydrogen generation rate (HGR) of 3,260 $mL \cdot min^{-1} \cdot g^{-1}_{cat.}$ at 30 ℃. Wang et al. [39] loaded Co-Mo-B nanoparticles on nickel foam by chemical deposition. The highest HGR of NH_3BH_3 hydrolysis reached 5,331 $mL \cdot min^{-1} \cdot g^{-1}_{cat.}$ at 30 ℃, and the reaction activation energy is 45.5 $kJ \cdot mol^{-1}$. Zhang et al. [40] loaded CoPt-Co on amino-modified SiO_2 nanospheres by chemical reduction method. The reaction activation energy is 37.05 $kJ \cdot mol^{-1}$ when catalyzing the hydrolysis of NH_3BH_3 aqueous solution. Sait Izgi et al. [35] supported Co-Fe-Ru-B catalyst for the first time with epoxy-activated acrylic particulate polymer, which catalyzed the hydrolysis of NH_3BH_3 with a HGR of 36,978 $mL \cdot min^{-1} \cdot g^{-1}_{cat.}$ at 30 ℃.

In our previous work, xSB-AB with different mole ratio was obtained by ball milling. The HGR of the composite is better than that of SB and AB monomer. However, the hydrogen release performance at 0-50 ℃ is not improved significantly [5]. Herein, in order to improve its hydrogen release performance under mild conditions, a simple and easily available CCH was used

as the catalyst for the hydrolysis of the composite. It is found that the addition of CCH can further significantly improve the hydrogen release performance of xSB-AB. What's more, the effect of catalyst addition method, molar ratio of SB to AB, catalyst addition amount, ratio of water to material and reaction temperature on the hydrogen release performance of xSB-AB were studied. Under the optimized conditions, the HGR of the composite was 299.32 $mL \cdot min^{-1} \cdot g^{-1}$, the hydrogen release efficiency (HRE) was 85.78% and the reaction activation energy was 62.12 $kJ \cdot mol^{-1}$. Fig. 1 shows a schematic diagram of the preparation and hydrolysis reaction of hydrolysis raw materials under optimized conditions. As a result, CCH has good catalytic effect for the hydrolysis system of 4SB-AB in the mild external conditions. CCH catalyzed hydrolysis of xSB-AB provides an effective way for the design and development of solid hydrogen storage materials, which is of great significance for developing clean energy.

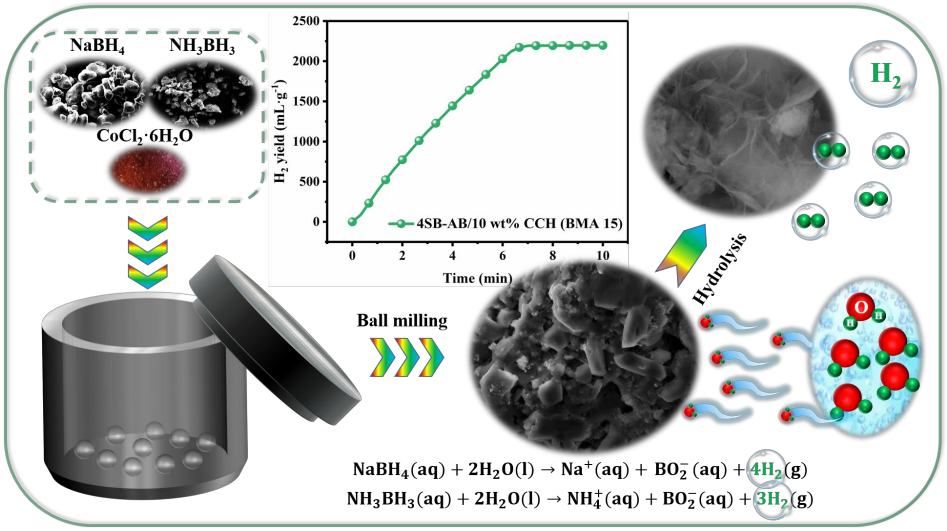

Fig. 1. Schematic diagram of preparation and hydrolysis reaction of hydrolysis raw materials under optimized conditions.

2. Experiment

2.1. Materials

In this experiment, $NaBH_4$ (98.0%), $CoCl_2 \cdot 6H_2O$ (99.99%), $(NH_4)_2SO_4$ (97.0%) were purchased from Chengdu City Cologne Chemical Co., Ltd. They were all analytically pure and were used as received. NH_3BH_3 was prepared with $NaBH_4$ and $(NH_4)_2SO_4$ as raw materials according to reference [41], and its purity was about 90%.

2.2. Preparation of hydrolysis raw materials

xSB-AB was prepared by Spex8000 ball mill machine at 400 $r \cdot s^{-1}$, and the weight ratio of ball to material was 30:1 [42]. The catalyst CCH was added using two different methods. Weighing a certain amount of CCH and adding it directly to xSB-AB was called direct addition (DA). A certain amount of CCH was weighed and ball-milled together with SB and AB (the molar ratio of SB and AB is x=2, 4, 6, 8), which was called ball milling addition (BMA). The hydrolysis raw material prepared by BMA method was expressed as xSB-AB/yCCH (BMA t), where y is the

catalyst addition amount (wt%) and t is the ball milling time (min). All loading and sampling operations in the experiment were completed in an argon atmosphere glove box (Dellix-5611101) with a purity of 99.9%. The O_2 content in the glove box was <0.1 ppm and the H_2O content was <0.1 ppm.

2.3. Hydrolysis experiments and hydrolyzed product collection

The hydrogen release kinetics was tested using the hydrolysis experimental device based on the drainage gas gathering method as described in our previous work [5] and the hydrolysis experimental steps described below. Put the round-bottom flask containing 0.2 g of hydrolysis raw material into the water bath, then connect it to the hydrolysis experimental device, and check the air tightness. Strat stirring, then inject a certain volume of deionized water into the flask at a rate of 100 $mL \cdot h^{-1}$, and record the volume of hydrogen released from the reaction. The deionized water injected into the flask was controlled to be 5, 10, 15, 20 mL, and the corresponding ratio of water to material were 25, 50, 75 and 100 $mL \cdot g^{-1}$, respectively. In order to ensure the accuracy of the experimental data, each group of experiments was repeated at least three times, and all the recorded hydrogen volumes were converted to the volume at 25 °C using the ideal gas equation, and then the average value was used.

After the hydrolysis experiment, the hydrolyzed product was collected and filtered in the air. The obtained black precipitate was placed in a vacuum drying oven to fully dry and obtained a black powder.

2.4. Composition and microstructure analysis

The composition of hydrolysis raw materials and hydrolyzed product was analyzed by X-ray diffractometer (XRD, DX-2700B, Liaoning Dandong Haoyuan Instrument Co., Ltd.), and the microstructure was analyzed by scanning electron microscope (SEM, FEI Inspect F50 and COXEM), and elemental mapping (SEM-Mapping) was analyzed by OXFORD ULTIM Max65. The test conditions of XRD were Cu Kα radiation, graphite monochromator, tube voltage of 40 kV, tube current of 30 mA, scanning range of 10° to 80°, step angle of 0.02° and sampling time of 1 s.

3. Results and discussion

3.1. Structure and micro-morphology of hydrolysis raw materials

Our previous studies have shown that the hydrolysis of 4SB-AB generally has better hydrogen release performance than other xSB-AB (x = 2, 6, 8) [42, 43]. Therefore, it was used as the initial object for the study of SB-AB hydrolysis catalyzed by CCH. XRD data in Fig. 2a shows that 4SB-AB/10 wt%CCH (BMA 15) was composed of SB (JCPDS NO. 01-074-1891), AB (JCPDS NO. 00-013-0292) and a small amount of CCH, indicating that no chemical reaction occurred during its preparation. EDS results shows that the weight ratio of Na, Co and Cl elements in 4SB-AB/10 wt%CCH (BMA 15) was 49.65, 3.60 and 3.13 wt% (Fig. 2e), which was basically consistent with the theoretical weight ratio 45.32, 2.48 and 2.98 wt%. However, the content of oxygen element was significantly higher than the theoretical value, which may be due to the deliquescence of 4SB-AB/10 wt%CCH (BMA 15) during storage, transportation and testing. Fig. 2f shows the elemental mapping of 4SB-AB/10 wt%CCH (BMA 15) by SEM, indicating that it

consists of O, Na, Cl and Co (consistent with the EDS results), among which Na, Cl, and Co were uniformly distributed whereas O was irregularly clustered due to deliquescence. SEM image in Fig. 2b shows that 4SB-AB/10 wt%CCH (BMA 15) was a polygonal columnar crystal structure with a length of 6-8 μm and 2-3 μm in diameter, which was quite different from the raw materials SB and AB. SB was mainly composed of 100-300 μm particles (Fig. 2c), while AB was mainly composed of 100-200 μm irregular blocks (Fig. 2d). The large reduction of particle size is expected to be beneficial to its hydrolysis reaction, as it implies a large increase in surface area and activity.

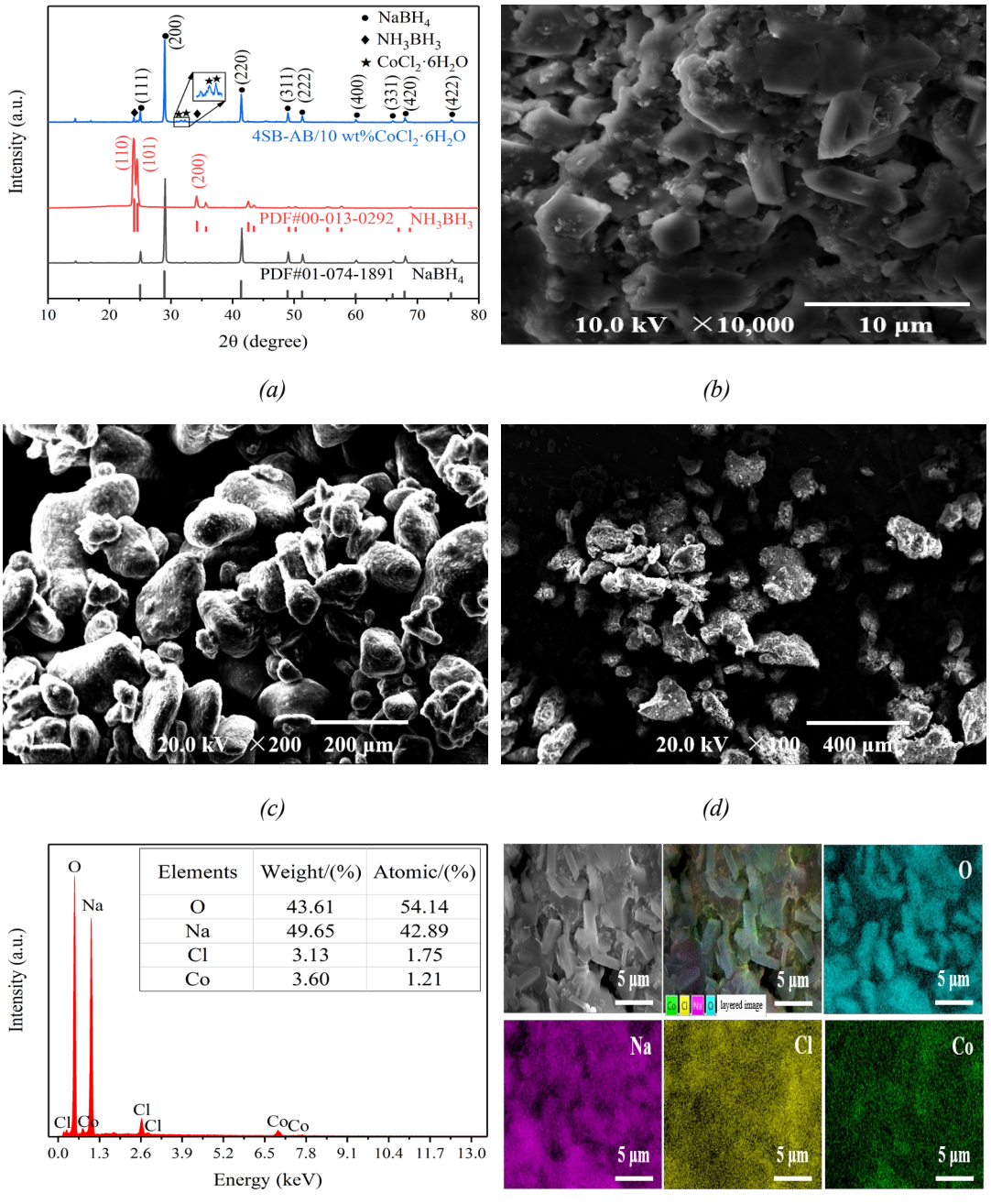

(a) *(b)*

(c) *(d)*

(e) *(f)*

Fig. 2. (a) XRD patterns of SB, AB and 4SB-AB/10 wt%CCH (BMA 15); SEM images of (b) 4SB-AB/10 wt%CCH (BMA 15), (c) SB and (d) AB; (e-f) EDS analysis and elemental mapping of 4SB-AB/10 wt%CCH (BMA 15) by SEM.

3.2. Hydrogen release performance

The hydrolysis hydrogen release kinetic curves in Fig. 3a show that 4SB-AB/yCCH prepared by BMA method has a faster HGR and higher HY than DA method when the CCH addition amount y is the same, which may be mainly attributed to 4SB-AB/yCCH prepared by BMA method has much smaller particle size (Fig. 2b-d). It can also be seen from Fig. 3a that the HGR of 4SB-AB/10 wt%CCH (BMA 15) was close to that of 4SB-AB/15 wt%CCH (BMA 15) and much faster than that of 4SB-AB/5 wt%CCH (BMA 15). In terms of HY, 4SB-AB/10 wt%CCH (BMA 15) was between 4SB-AB/5 wt%CCH (BMA 15) and 4SB-AB/15 wt%CCH (BMA 15), and their HY were 2,194.01, 2,369.95 and 1,906.64 $mL \cdot g^{-1}$, respectively. Therefore, 4SB-AB/10 wt%CCH (BMA) was selected to study the effect of ball milling time on the hydrogen release performance.

Fig. 3b shows the hydrolysis hydrogen release kinetic curves of 4SB-AB/10 wt%CCH after different ball milling time. It could be seen that when the ball milling time was changing between 15 and 60 min, the HGR of 4SB-AB/10 wt%CCH decreases gradually with the increase of ball milling time. When the ball milling time was set as 15, 30, 60 min, the HGR of 4SB-AB/10 wt%CCH were 299.32, 289.91 and 209.02 $mL \cdot min^{-1} \cdot g^{-1}$, respectively. And the HY were 2,194.01, 2,029.35 and 2,439.21 $mL \cdot g^{-1}$, respectively. Although the HY of 4SB-AB/10 wt%CCH (BMA 15) was lower than that of 4SB-AB/10 wt%CCH (BMA 60), the HGR of 4SB-AB/10 wt%CCH (BMA 15) was highest. It is possibly caused by the synergistic effect of SB and AB after ball milling for different times. At the same time, long-time ball milling will consume more energy. Therefore, xSB-AB/10 wt%CCH (BMA 15) was selected to study the effect of molar ratio of SB to AB on the hydrogen release performance.

Our previous work have shown that the ratio of SB to AB in the SB-AB composite hydrolysis system has an important effect on the hydrogen release performance [43]. Therefore, we investigated the effect of different molar ratios of SB and AB on the hydrogen release performance of SB-AB/10 wt%CCH (BMA 15) (Fig. 3c). When the molar ratio of SB to AB increased from 2 to 8, the HGR of xSB-AB/10 wt%CCH (BMA 15) increased first and then decreased, shows a non-linear trend. Among them, 4SB-AB/10 wt%CCH (BMA 15) has the best hydrogen release performance, and its HGR and HY were 299.32 $mL \cdot min^{-1} \cdot g^{-1}$ and 2,194.01 $mL \cdot g^{-1}$, respectively. When x=4, 6, 8, here was little difference in HY of the composite, the HY were 2,194.01, 2,149.62 and 2,230.10 $min^{-1} \cdot g^{-1}$, respectively. Therefore, 4SB-AB/yCCH (BMA 15) was selected to study the effect of CCH addition amount on the hydrogen release performance.

Fig. 3d shows the effects of CCH addition amount on the hydrogen release performance of xSB-AB/yCCH. It can be seen that when the CCH addition amount increased from 5wt% to 15wt%, the HGR of 4SB-AB/yCCH (BMA 15) showed an overall increasing trend, while the HY of SB-AB/yCCH (BMA 15) showed an overall decreasing trend. This indicates that too much or too little catalyst will affect the hydrogen release performance. This may be because the proportion of reactant decrease with the increase of catalyst addition amount, or the reactant and catalyst cannot fully contact with each other under the condition of less catalyst addition amount. In a series of 4SB-AB/yCCH (BMA 15) reaction systems, 4SB-AB/10 wt%CCH (BMA 15) has high HGR and HY, which were 299.32 $mL \cdot min^{-1} \cdot g^{-1}$ and 2,194.01 $mL \cdot g^{-1}$, respectively. Therefore, 4SB-AB/10 wt%CCH (BMA 15) was selected to study the effect of ratio of water to material and reaction temperature the hydrogen release performance.

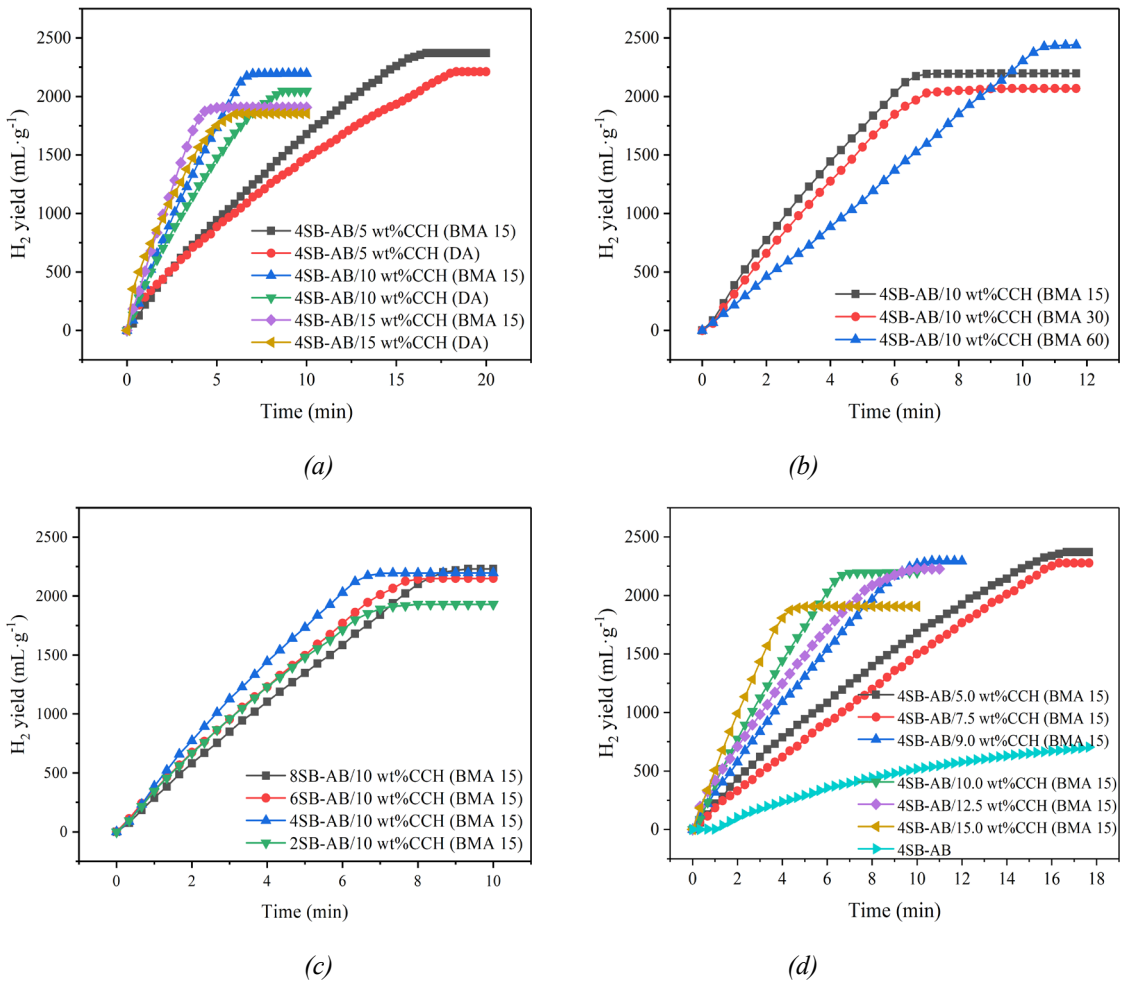

Fig. 3. Effects of (a) CCH addition method, (b) ball milling time, (c) molar ratio of SB to AB and (d) CCH addition amount on the hydrogen release performance of xSB-AB/yCCH hydrolysis. The reaction temperature was 40 ℃, and the ratio of water to material was 50 mL·g^{-1}.

Fig. 4a shows that the ratio of water to material has a great impact on the hydrogen release performance of 4SB-AB/10 wt%CCH (BMA 15). When the ratio of water to material increases from 25 mL·g^{-1} to 100 mL·g^{-1}, the HGR and HY of the composite shows a non-linear trend. When the ratio of water to material was 50 mL·g^{-1}, the HGR of 4SB-AB/10 wt%CCH (BMA 15) was the fastest, which was 299.32 mL·min^{-1}·g^{-1}. When the ratio of water to material was 25 and 100 mL·g^{-1}, the initial hydrogen release curve trend of the composite was similar, with HY of 2,343.95 and 2,322.70 mL·g^{-1}, respectively. However, their HGR were 200.90 and 148.26 mL·min^{-1}·g^{-1}, respectively, which was obviously lower than that when the ratio of water to material was 50 mL·g^{-1}. The results show that the ratio of water to material of 50 mL·g^{-1} was the best choice for the composite.

The reaction rates at different reaction temperature determined the application environment of hydrolysis system. Finally, we studied the effect of reaction temperature (T=10-60 ℃) on the hydrogen release performance of 4SB-AB/10 wt%CCH (BMA 15). Hydrolysis data in Fig. 4b and Table 1 shows that the reaction rate can be improved significantly

by increasing reaction temperature. When the reaction temperature was 10 °C, the HGR of 4SB-AB/10 wt%CCH (BMA 15) was slow and about 18.84 mL·min^{-1}·g^{-1}. When the temperature was higher than 30 ℃, the hydrolysis rate increased significantly. When T=40 ℃, the HGR can reach 299.32 mL·min^{-1}·g^{-1}, which was 15.89 times of that when T=10 ℃. Although the HGR can be further improved when T=50 and 60 ℃, the improvement effect was not so obvious and the HRE were nearly equivalent. Hence in order to reduce the energy consumption of the hydrolysis reaction, 40 ℃ as the appropriate temperature for the hydrolysis of the composite. Of course, the hydrolysis of 4SB-AB/10 wt%CCH (BMA 15) also has good performance when the reaction temperature was close to room temperature (for example, when the T=20 ℃ and 30 ℃, the HGR was 42.16 and 150.94 mL·min^{-1}·g^{-1}), as shown in Table 1.

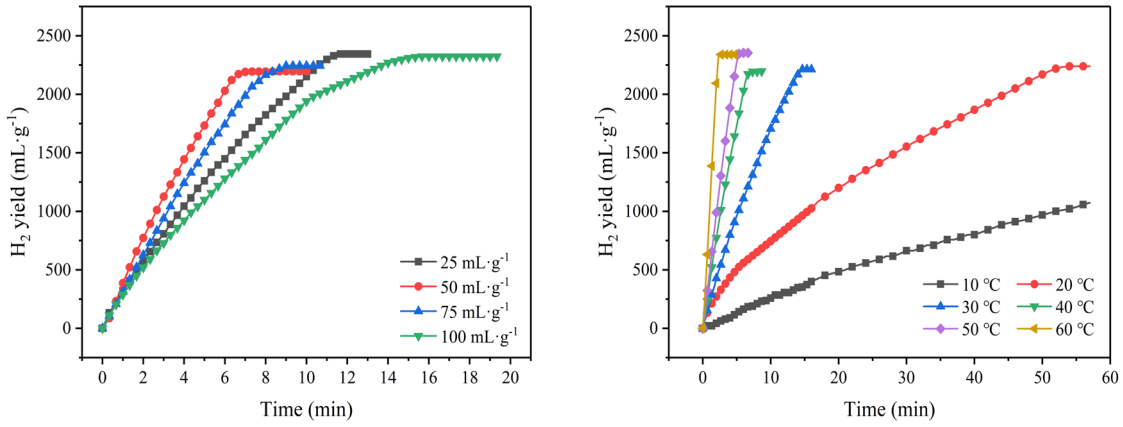

Fig. 4. Effects of (a) ratio of water to material and (b) reaction temperature on the hydrogen release performance of 4SB-AB/10 wt%CCH (BMA 15) hydrolysis.

Table 1. HY, HGR and HRE of composite with different of temperature.

Temperature/(℃)	10	20	30	40	50	60
HY/(mL·g^{-1})	~1,074.00	2,234.31	2,212.90	2,194.01	2,345.70	2,339.50
HGR/(mL·min^{-1}·g^{-1})	~18.84	42.16	150.94	299.32	440.10	1,004.08
HRE/(%)	~42.00	87.36	86.52	85.78	91.71	91.47

Note: HGR, hydrogen generation rate; HY, Hydrogen yield; HRE, hydrogen release efficiency.
HGR= HY/Stable time, HRE= Actual hydrogen yield/Theoretical hydrogen yield.

3.3. Hydrolyzed product analysis

XRD data in Fig. 5a shows that hydrolyzed product has no obvious diffraction peak and exhibits amorphous characteristics. This may be caused by the morphology and structure of the hydrolyzed product presenting a special amorphous "thin film" like substance (Figs. 5b-c). In order to further analyze the composition of hydrolyzed product, EDS was used to perform elemental

detection and analysis on different regions, and the results were shown in Figs. 5e-g. EDS results shows that the main element composition of hydrolyzed product was Co and O, and their average weight percentage was about 50.16 wt% and 35.07 wt%, respectively (Figs. 5e-g). In addition, their average atomic percentage was about 20.74% and 51.29%, respectively. This indicates that the hydrolyzed product with amorphous "thin film" substance may be Co oxide.

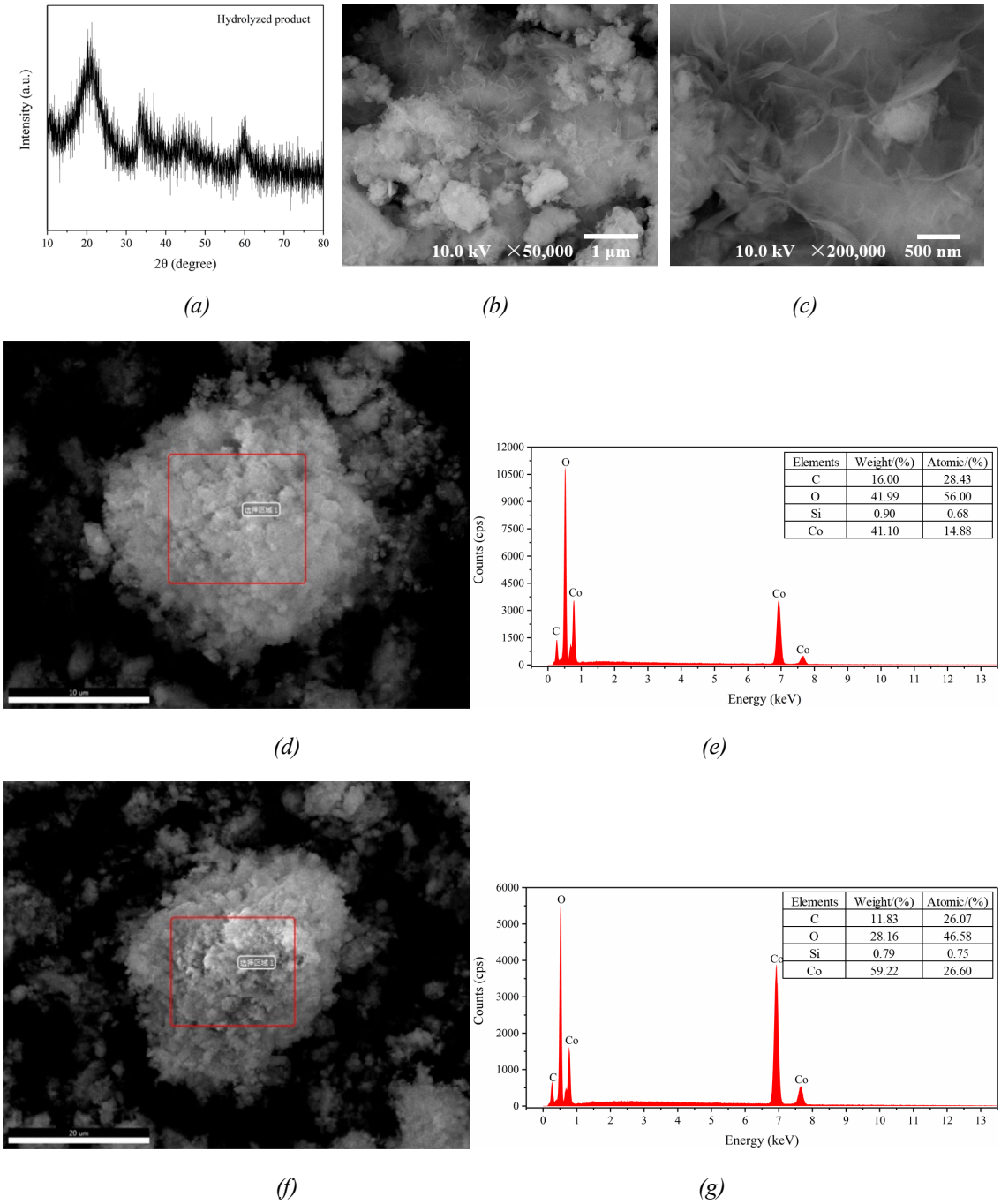

Fig. 5 (a) XRD patterns and (b-c) SEM images of hydrolyzed product; EDS analysis of hydrolyzed product in (d-e) region 1 and (f-g) region 2.

3.4. Activation energy (E_a) of the reaction

As shown in Fig. 4b, under the action of CCH catalyst, the hydrolysis rate of SB-AB increases with the increase of reaction temperature. At each reaction temperature, HY has a linear relationship with the reaction time, this means that the reaction is of zero order [44]. Therefore, Arrhenius equation (Formula (3)) can be used to determine the activation energy (E_a) of the reaction [33, 44-48].

The E_a is calculated by the Arrhenius formula:

$$k=A \exp(-E_a/RT) \quad (3)$$

In the formula (3), k is the reaction rate constant, T is the reaction temperature, A is the pre-exponential factor, R is the ideal gas constant and E_a is the activation energy of the reaction. Formula (4) can be obtained from the evolution of formula (3).

$$\ln k=\ln A-(E_a/R)\cdot(1/T) \quad (4)$$

Fig. 6 shows the Arrhenius plot (ln k versus reciprocal absolute temperature 1/T) and HGR values for hydrolysis reaction of 4SB-AB/10 wt%CCH (BMA 15). The E_a of the reaction was calculated from the slope of the fitted line was 62.12 kJ·mol^{-1}, and the correlation coefficient R^2 was 0.98186. Compared with other Co-based catalysts (Table 2), although the E_a obtained in our experiment is not too low, the good hydrogen release performance of 4SB-AB/10 wt%CCH (BMA 15) at different temperatures still indicates that it has a relatively ideal hydrogen release kinetics.

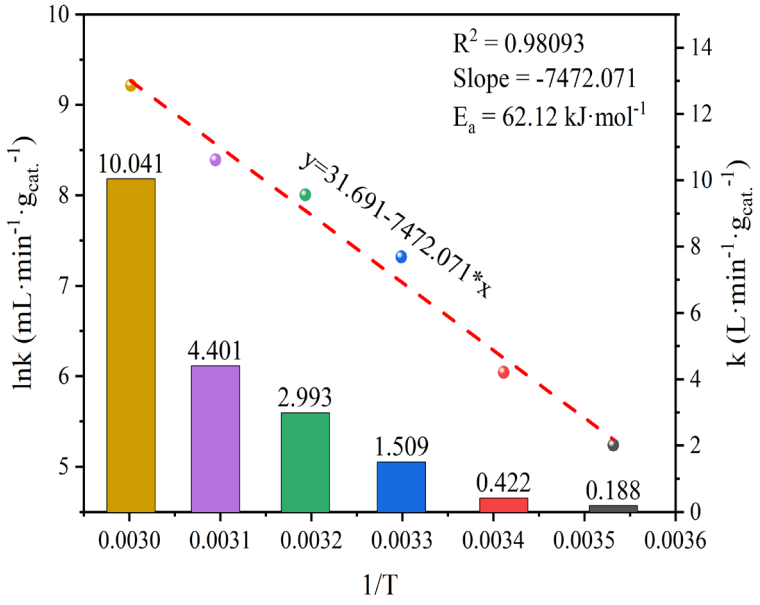

Fig. 6 Arrhenius plot (ln k versus reciprocal absolute temperature 1/T) and HGR values for hydrolysis reaction of 4SB-AB/10 wt%CCH (BMA 15).

Table 2. Comparison of the catalytic activity and activation energy of various catalysts.

Catalyst	Reactants	Catalytic activity		Activation energy test		Ref.
		T/(℃)	HGR	RT/(℃)	E_a/(kJ·mol^{-1})	
CCH	4SB-AB/10 wt%CCH (BMA 15)	40	2,993.2	10-60	62.12	This work
Co/HTNT	2.5 wt%$NaBH_4$ + 12.5 wt%NaOH	40	1,320	20-50	29.68 ± 2.24	[49]
Co/IR-120	5 wt%$NaBH_4$ + 5 wt%NaOH	35	200	20-50	66.67	[50]
Co-Cr-B/γ-Al_2O_3	0.31 wt%NH_3BH_3 + 3 wt%NaOH	30	3,260	30-60	56.06	[38]
CCH	4SB-AB/10 wt%CCH (BMA 15)	30	1,509.4	10-60	62.12	This work
p(AMPS)-Co	50 mM $NaBH_4$ + 5 wt%NaOH	30	937.5	30-70	38.14	[29]
CNSs@$Pt_{0.1}Co_{0.9}$	~1 wt%$NaBH_4$ + 1 wt%NaOH	30	8,943	25-45	38	[51]
Co-Cr-B/CeO_2	2.5 wt%$NaBH_4$ + 3 wt%NaOH	30	9,182	30-60	35.52	[52]
Co/HTNT	2.5 wt%$NaBH_4$ + 12.5 wt%NaOH	30	1,040	20-50	29.68 ± 2.24	[49]
CoB/Sepiolite	5 wt%$NaBH_4$ +1 wt%NaOH	30	1,486	30-60	21.4	[53]
Pd/Co_3O_4	10 wt%$NaBH_4$ + 1 wt%NaOH	25	2,109	25-55	65.82	[54]
Co(0)-HAP	7.47 mmol $NaBH_4$	25	5,000	15-45	53 ± 2	[55]
	2 mmol NH_3BH_3		2,000	25-45	50 ± 2	
Co-P/CNTs-NF	10 wt%$NaBH_4$ + 1 wt%NaOH	25	2,430	25-40	49.94	[56]
Co-Mo-B/NF	NH_3BH_3 solution	25	5,331	25-45	45.5	[39]
Zr-Ni-B	Solid $NaBH_4$	25	384.2	25-45	45.23	[57]
Co/NF	~3.8 wt%$NaBH_4$ + 4.5 wt%NaOH	23	2,650	25-40	60 ± 2	[58]
Co-B	20 wt%$NaBH_4$ + 5 wt%NaOH	20	875	10-30	68.87	[59]
CCH	4SB-AB/10 wt%CCH (BMA 15)	20	414.7	10-60	62.12	This work
Raney Co	1 wt%$NaBH_4$ + 10 wt%NaOH	20	267.5	20-40	53.7	[60]
(CoP NA/Ti)	1 wt%$NaBH_4$ + 1 wt%NaOH	20	6,500	10-50	41	[61]
Co/HTNT	2.5 wt%$NaBH_4$ + 12.5 wt%NaOH	20	660	20-50	29.68 ± 2.24	[49]
Co_2B	1 wt%$NaBH_4$ + 10 wt%NaOH	20	468.3	—	—	[60]
CoCl2/γ-Al_2O_3	2 wt%$NaBH_4$ + x wt%NaOH	—	—	20-40	132	[36]
				50-65	78	

Catalyst	Reactants	Catalytic activity		Activation energy test		Ref.
		T/(℃)	HGR	RT/(℃)	E_a/(kJ·mol^{-1})	
Pt/$LiCoO_2$	10% $NaBH_4$ + 5% NaOH	—	—	25-40	70.4	[62]
Co/γ-Al_2O_3	1 wt%NH_3BH_3	—	—	20-40	62	[63]
Pd/C	1 mmol NH_3BH_3	—	—	30-45	57.92	[64]
Co-Pd/C					35.7	
PVP-stabilized Ru-Pd NPs	0.375 M $NaBH_4$	—	—	15-35	52.5±2	[65]
	0.1 M NH_3BH_3			10-30	54.2±2	
CoCl2/AC	2 wt%NaBH4 + x wt%NaOH	—	—	20-60	48	[37]
SiO2@Pt0.1Co0.9	1.5 mmol NH3BH3	—	—	25-45	37.05	[40]

Note: HGR, hydrogen generation rate, the unit is mL·min-1·g-1cat.; RT, Reaction temperature; Ea, Activation energy; Ref., Reference; HTNT, hydrogen titanate nanotubes; AMPS, 2-acrylamido-2-methyl-1-propansulfonic acid; CNSs, carbon nanospheres; rGO, reduced graphene oxide; EP, Epoxy-activated acrylic particulate polymer; NF, Nickel foam; HAP, Hydroxyapatite; CNTs, carbon nanotubes; NA, nanowire array; NPs, nanoparticles; AC, activated carbon.

4. Conclusion

In this study, CCH was used as an effective catalyst for catalyzing the hydrolysis of xSB-AB. The major factors influencing the hydrogen release performance of xSB-AB were systematically studied. The hydrolysis of the composite system showed a best performance when a mass percentage of 10 wt% was adapted for CCH in the composite, the ball milling time was 15 min and the reaction temperature was kept at 40 ℃. The HGR was 299.32 mL·min^{-1}·g^{-1} and the HY can reach 2,194.01 mL·g^{-1}. The reaction activation energy was 62.12 kJ·mol^{-1}. Due to the advantages of CCH catalyzing hydrolysis of xSB-AB under mild reaction conditions, it has a high potential in the field of hydrogen energy production.

Acknowledgements

This work was supported by the Open Fund of Engineering Research Center of Alternative Energy Materials & Devices (grant number AEMD202203); the Chengdu University Talent Engineering Research Start-up Project (grant number 2081921083), the National Natural Science Foundation of China (grant number. 21805046, 22179024), the Science and Technology Plan Project of Guangzhou City (grant number 202102020426), the Open Fund of the Guangdong Provincial Key Laboratory of Advanced Energy Storage Materials, South China University of Technology (grant number AESM202111), Project of "One-Hundred Young Talents" of Guangdong University of Technology (grant number 220413551).

References

[1] W. Chen et al. Journal of Power Sources **359**, 400 (2017); https://doi.org/10.1016/j.jpowsour.2017.05.075

[2] J. L. Zhu et al. Digest Journal of Nanomaterials and Biostructures **17**(3), 799 (2022); https://doi.org/10.15251/djnb.2022.173.799

[3] M. Mîndroiu et al. Digest Journal of Nanomaterials and Biostructures **17**(3), 999 (2022); https://doi.org/10.15251/djnb.2022.173.999

[4] S. B. Kalidindi et al. Phys Chem Chem Phys **10**(38), 5870 (2008); https://doi.org/10.1039/b805726e

[5] Z. Huang et al. International Journal of Hydrogen Energy **37**(6), 5137 (2012); https://doi.org/10.1016/j.ijhydene.2011.12.033

[6] P. P. Edwards et al. Philos Trans A Math Phys Eng Sci **365**(1853), 1043 (2007); https://doi.org/10.1098/rsta.2006.1965

[7] W.-Z. Gai et al. Sustainable Energy Technologies and Assessments **38**, 100676.1 (2020); https://doi.org/10.1016/j.seta.2020.100676

[8] Q. Yao et al. Inorganic Chemistry Frontiers **7**(20), 3837 (2020); https://doi.org/10.1039/d0qi00766h

[9] Z. Wen et al. Nanomaterials (Basel) **10**(8), (2020); https://doi.org/10.3390/nano10081612

[10] M. Paladini et al. Applied Catalysis B: Environmental **210**, 342 (2017); https://doi.org/10.1016/j.apcatb.2017.04.005

[11] M. Yang et al. Digest Journal of Nanomaterials and Biostructures **18**(2), 495 (2023); https://doi.org/10.15251/djnb.2023.182.495

[12] H.-L. Jiang et al. Catalysis Today **170**(1), 56 (2011); https://doi.org/10.1016/j.cattod.2010.09.019

[13] A. Kantürk Figen et al. International Journal of Hydrogen Energy **38**(6), 2824 (2013); https://doi.org/10.1016/j.ijhydene.2012.12.067

[14] W. Chen et al. Chem Commun (Camb) **50**(17), 2142 (2014); https://doi.org/10.1039/c3cc48027e

[15] F. Toche et al. International Journal of Hydrogen Energy **37**(8), 6749 (2012); https://doi.org/10.1016/j.ijhydene.2012.01.037

[16] M. Soltani et al. International Journal of Hydrogen Energy **45**(22), 12331 (2020); https://doi.org/10.1016/j.ijhydene.2020.02.203

[17] D. Xu et al. J Colloid Interface Sci **516**, 407 (2018); https://doi.org/10.1016/j.jcis.2018.01.061

[18] Z.-H. Lu et al. Journal of Materials Chemistry **22**(11), (2012); https://doi.org/10.1039/c2jm14787d

[19] H. Chu et al. International Journal of Hydrogen Energy **44**(3), 1774 (2019); https://doi.org/10.1016/j.ijhydene.2018.11.101

[20] Y. Liu et al. Advanced Sustainable Systems **3**(5), (2019); https://doi.org/10.1002/adsu.201800161

[21] X. Qiu et al. RSC Advances **10**(17), 9996 (2020); https://doi.org/10.1039/d0ra01720e

[22] Q. Yao et al. International Journal of Hydrogen Energy **40**(5), 2207 (2015); https://doi.org/10.1016/j.ijhydene.2014.12.047

[23] H. Liu et al. International Journal of Hydrogen Energy **44**(31), 16548 (2019); https://doi.org/10.1016/j.ijhydene.2019.04.200
[24] X. Zhang et al. ACS Appl Mater Interfaces **12**(8), 9376 (2020); https://doi.org/10.1021/acsami.9b22645
[25] T. E. Bell et al. Topics in Catalysis **59**(15-16), 1438 (2016); https://doi.org/10.1007/s11244-016-0653-4
[26] U. B. Demirci et al. Phys Chem Chem Phys **16**(15), 6872 (2014); https://doi.org/10.1039/c4cp00250d
[27] Y.-J. Shih et al. Energy **54**, 263 (2013); https://doi.org/10.1016/j.energy.2013.01.063
[28] Ö. Şahin et al. Reaction Kinetics, Mechanisms and Catalysis **133**(2), 851 (2021); https://doi.org/10.1007/s11144-021-02004-w
[29] N. Sahiner et al. Applied Catalysis B: Environmental **102**(1-2), 201 (2011); https://doi.org/10.1016/j.apcatb.2010.11.042
[30] J. Zhu et al. Journal of Power Sources **211**, 33 (2012); https://doi.org/10.1016/j.jpowsour.2012.03.051
[31] D. G. Tong. RSC Advances **10**(21), 12354 (2020); https://doi.org/10.1039/d0ra90028a
[32] Y. Wang et al. International Journal of Hydrogen Energy **45**(16), 9845 (2020); https://doi.org/10.1016/j.ijhydene.2020.01.157
[33] Ö. Şahin et al. Graphene Technology **5**(3-4), 103 (2020); https://doi.org/10.1007/s41127-020-00036-y
[34] H. Ç. Kazıcı et al. Chemical Papers **75**(6), 2713 (2021); https://doi.org/10.1007/s11696-021-01514-0
[35] M. S. İzgi et al. International Journal of Hydrogen Energy **45**(43), 22638 (2020); https://doi.org/10.1016/j.ijhydene.2020.06.048
[36] Ç. Çakanyıldırım et al. Renewable Energy **35**(4), 839 (2010); https://doi.org/10.1016/j.renene.2009.08.034
[37] Ç. Çakanyıldırım et al. International Journal of Green Energy **14**(12), 1005 (2017); https://doi.org/10.1080/15435075.2017.1354297
[38] M. Sait Izgi et al. Materials and Manufacturing Processes **34**(14), 1620 (2019); https://doi.org/10.1080/10426914.2019.1594280
[39] Y. Wang et al. International Journal of Hydrogen Energy **44**(21), 10508 (2019); https://doi.org/10.1016/j.ijhydene.2019.02.157
[40] H. Zhang et al. Progress in Natural Science: Materials International **29**(1), 1 (2019); https://doi.org/10.1016/j.pnsc.2019.01.001
[41] P. V. Ramachandran et al. Inorg Chem **46**(19), 7810 (2007); https://doi.org/10.1021/ic700772a
[42] Y. Xu et al. International Journal of Hydrogen Energy **41**(37), 16344 (2016); https://doi.org/10.1016/j.ijhydene.2016.05.234
[43] Y. Xu et al. Journal of Power Sources **261**, 7 (2014); https://doi.org/10.1016/j.jpowsour.2014.03.038
[44] H. Çelik Kazici et al. Journal of Electronic Materials **49**(6), 3634 (2020); https://doi.org/10.1007/s11664-020-08061-6
[45] C. Cui et al. Applied Catalysis B: Environmental **265**, (2020); https://doi.org/10.1016/j.apcatb.2020.118612

[46] H. Ç. Kazıcı et al. Journal of Electronic Materials **51**(5), 2356 (2022); https://doi.org/10.1007/s11664-022-09491-0
[47] E. Onat et al. Journal of Materials Science: Materials in Electronics **32**(23), 27251 (2021); https://doi.org/10.1007/s10854-021-07094-9
[48] E. Onat et al. Journal of the Australian Ceramic Society **57**(5), 1389 (2021); https://doi.org/10.1007/s41779-021-00643-9
[49] R. Li et al. International Journal of Hydrogen Energy **47**(8), 5260 (2022); https://doi.org/10.1016/j.ijhydene.2021.11.143
[50] C.-H. Liu et al. Applied Catalysis B: Environmental **91**(1-2), 368 (2009); https://doi.org/10.1016/j.apcatb.2009.06.003
[51] H. Zhang et al. Applied Surface Science **540**, (2021); https://doi.org/10.1016/j.apsusc.2020.148296
[52] M. S. İzgi et al. International Journal of Hydrogen Energy **45**(60), 34857 (2020); https://doi.org/10.1016/j.ijhydene.2020.04.034
[53] N. Selvitepe et al. International Journal of Hydrogen Energy **44**(31), 16387 (2019); https://doi.org/10.1016/j.ijhydene.2019.04.254
[54] G. Bozkurt et al. Energy **180**, 702 (2019); https://doi.org/10.1016/j.energy.2019.04.196
[55] M. Rakap et al. Catalysis Today **183**(1), 17 (2012); https://doi.org/10.1016/j.cattod.2011.04.022
[56] F. Wang et al. International Journal of Hydrogen Energy **43**(18), 8805 (2018); https://doi.org/10.1016/j.ijhydene.2018.03.140
[57] D. Lim et al. International Journal of Hydrogen Energy **47**(5), 3396 (2022); https://doi.org/10.1016/j.ijhydene.2021.03.039
[58] M. Paladini et al. Applied Catalysis B: Environmental **158-159**, 400 (2014); https://doi.org/10.1016/j.apcatb.2014.04.047
[59] S. U. Jeong et al. Journal of Power Sources **144**(1), 129 (2005); https://doi.org/10.1016/j.jpowsour.2004.12.046
[60] B. H. Liu et al. Journal of Alloys and Compounds **415**(1-2), 288 (2006); https://doi.org/10.1016/j.jallcom.2005.08.019
[61] L. Cui et al. Nano Research **10**(2), 595 (2016); https://doi.org/10.1007/s12274-016-1318-0
[62] Z. Liu et al. Journal of Power Sources **176**(1), 306 (2008); https://doi.org/10.1016/j.jpowsour.2007.09.114
[63] Q. Xu et al. Journal of Power Sources **163**(1), 364 (2006); https://doi.org/10.1016/j.jpowsour.2006.09.043
[64] F. Xu et al. ACS Applied Nano Materials **4**(7), 7479 (2021); https://doi.org/10.1021/acsanm.1c01500
[65] M. Rakap. International Journal of Green Energy **12**(12), 1288 (2014); https://doi.org/10.1080/15435075.2014.895737